Deep Resources Engineering 3 (2026) 100205

Contents lists available at ScienceDirect

Deep Resources Engineering

journal homepage: www.keaipublishing.com/en/journals/deepre/

Full length article

Calculation model of overburden pressure of large diameter mounded storage tanks under different overburden slope angles

Zheng Nie [a,b], Yu Zhang [a,b,*], Shengjie Di [c], Chongqun Gao [a,b], Jiawei Lu [a,b], Jiajun Liu [a,b]

[a] State Key Laboratory of Intelligent Deep Metal Mining and Equipment, Northeastern University, Shenyang 110819, China

[b] Key Laboratory of Liaoning Province on Deep Engineering and Intelligent Technology, Northeastern University, Shenyang 110819, China

[c] Northwest Engineering Corporation Limited, Xi'an 710065, China

ARTICLE INFO

Keywords:
Large diameter mounded horizontal tanks
Covered with soil
Earth pressure
Improvement of the Marston model
Slope angle

ABSTRACT

Hazardous chemical horizontal tanks are widely used owing to their reliable storage capacity. To guarantee the safety and concealment of horizontal tanks, overburden is used to achieve effective isolation from adjacent heat sources, explosive shock waves or other unexpected damage. However, due to the large diameter of the mounded horizontal tanks, the earth pressure caused by different slope angles has a significant impact on the safety and stability of the tanks, and the earth pressure distribution and loads are different from the existing theoretical calculations, limitations of the earth pressure calculation method exist. In this paper, the "cat-ear" model and the "parabolic" model were established on the basis of Marston's theory, considering the factors of large diameter and different slopes. The model calculation results were compared and verified with the finite element results, and the parameter sensitivity analysis was carried out. The model can cover a variety of overburden heights and tank diameters in the case of earth pressure calculation, with high calculation accuracy and applicability, and can provide a reference for the structural design of overburden storage tanks and the formulation of specifications.

1. Introduction

Safety accidents caused by hazardous chemicals have occurred frequently and seriously in China [1]. Due to the characteristics of high pressure resistance, strong sealing and low cost, horizontal tanks are commonly used to store petrochemical fuels [2]. To meet the large number of storage needs and site constraints, storage tanks are usually centralized construction to form a large storage tank cluster, and hazardous chemicals have obvious heat-sensitive properties, once the rupture of its storage equipment is very easy to trigger a chain of explosions in the tank area. Therefore, the mound storage horizontal tanks can be used to prevent and reduce the occurrence of such accidents by covering the surface of the horizontal tanks with soil to form a protective layer. In addition, the mound storage horizontal tanks have the advantages of beautifying the environment, reducing the footprint, narrowing the distance with the surrounding adjacent facilities, and camouflaging the surrounding area for safety [3,4], thus attracting attention in China. The mounded storage horizontal tanks need to account the complex tank-soil interaction on the stability, the most important of which is the earth pressure generated by the soil covered tank instability, so the calculation of earth pressure on the top of the tank at different slope angles is the basis for the structural design of mounded storage tanks.

The load calculations of mounded storage horizontal tanks are often based on the EEMUA 190 [5] international guidelines, but there is no research report on the reliability of this method in China. Considering that the mounded storage horizontal tanks and buried pipeline to have the same cylindrical structure, the research method and theory of the buried pipeline earth pressure are adopted as the research basis in this paper. The earth pressure theory was firstly proposed by Marston and Anderson [6], and then modified by Spangler [7] (as documented in American Water Works Association). This theory assumes that the vertical and horizontal deformation of the pipe are equal, the earth pressure at the top and bottom of the pipe is simplified to be uniformly distributed, and the earth pressure at the side of the pipe is simplified to be parabolically distributed. However, the test proved that the earth pressure on the top of the pipe was not uniformly distributed, and the earth pressure in radial and tangential directions was approximately parabolic distribution [8], vertical earth pressure at the top of the pipe at low burial depth is mainly concentrated at the center of the pipe top, and becomes more and more obvious with the increase of the overburden height [9], while the vertical earth pressure at the top of the pipe at high burial depth is distributed in a "concave" shape [10,11]. And Zhou et al.

* Corresponding author at: State Key Laboratory of Intelligent Deep Metal Mining and Equipment, Northeastern University, Shenyang 110819, China.
E-mail address: zhangyu3@mail.neu.edu.cn (Y. Zhang).

https://doi.org/10.1016/j.deepre.2025.100205
Received 13 May 2025; Received in revised form 8 July 2025; Accepted 18 July 2025
Available online 21 July 2025

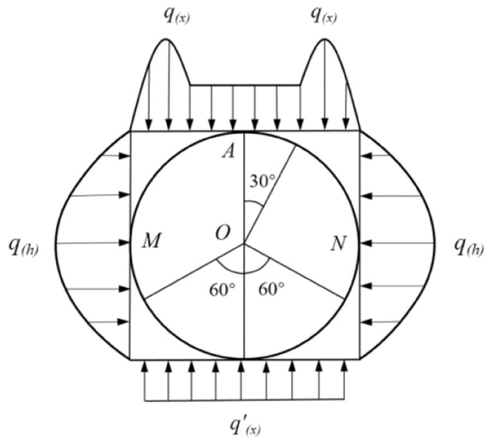

Fig. 1. "Cat-ear" earth pressure model.

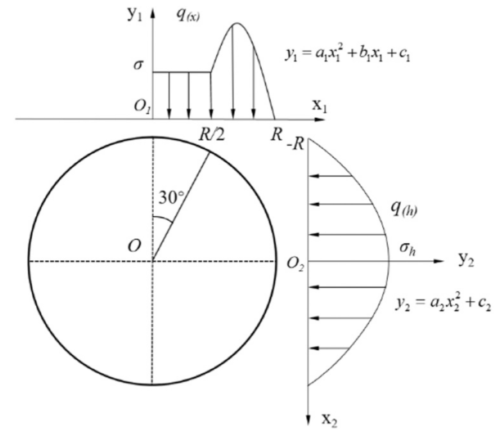

Fig. 2. Model calculation diagram.

[12,13] carried out numerical simulation studies on buried steel pipe, and obtained that the vertical and horizontal earth pressure around the pipe was roughly parabolic distribution. Yu et al. [14] obtained the vertical earth pressure distribution law of large-diameter pipe through finite element results, and proposed that there is a soil "chest" load around the large-diameter pipeline, and the large diameter of the pipeline will lead to a change in the distribution of storage tanks. Wang [15] proposed that the pipeline stress distribution is highly dependent on the distance of the buried pipeline from the slope and the resultant pipe-soil interaction. Comparing the earth pressure study of buried pipelines [16], the effect of earth arch effect on tank earth pressure; the effect of large diameter on tank load distribution and the effect of slope angle on tank earth pressure and load distribution were not considered in the load calculation of the existing mounded storage horizontal tanks. Therefore, it is necessary to carry out research on the calculation of earth pressure at the top of tanks with different slope angles.

In summary, the existing earth pressure theory is unreasonable in terms of earth arch effect, large diameter and slope angle, leading to unreliable earth pressure calculation model and unreasonable tank design, which in turn increases the risk of tank damage and instability. Therefore, this paper establishes the "cat-ear" model and the "parabolic" model on the basis of Marston theory, and discusses the influence of overburden height and tank diameter on this model. The model can be well suited for the calculation of earth pressure of large-diameter mounded storage horizontal tanks under different slope angles, which can provide important theoretical basis and technical support for the mounded storage horizontal tanks earth pressure calculation. The results of this study can ensure the safe and stable operation of deep underground energy storage projects.

2. Mounded storage horizontal tanks earth pressure model

2.1. Mounded storage horizontal tanks earth pressure model with angle $= 90^\circ$

The site tank project is oversized which will make monitoring inconvenient once construction is complete. Therefore, the earth pressure distribution on top of the tanks was analyzed using the numerical simulation results (Appendix A), which informed that the form of the earth pressure distribution was approximated as a cat-ear, and a new type of earth pressure calculation model was proposed based on this shape –the "cat-ear" model (Fig. 1).

The model adopts the shape of "horizontal line + parabola" to describe the earth pressure distribution of the mounded storage horizontal tanks: it is assumed that the vertical earth pressure is a certain value in the range from $\theta = 0^\circ$ to $\theta = 30^\circ$, and a parabolic distribution in the range from 30° to 90°, and the vertical earth pressure is 0 at $\theta = 90^\circ$; it is assumed that the lateral earth pressure as conforms to a parabolic distribution, the maximum value in the middle of the tank at $\theta = 90^\circ$ and the minimum values at the top of the tank at $\theta = 0^\circ$ and the bottom of the tank at $\theta = 180^\circ$.

The right half of the model is used as an example to calculate pressure distribution since the earth pressure distribution in the "cat-ear" model is symmetrical about the vertical axis of the tank center (Fig. 2).

Let the vertical earth pressure equation $q_{(x)}$ is $y_1 = a_1x_1^2 + b_1x_1 + c_1$, in the x_1–y_1 coordinate system, when $0 \le x_1 \le R/2$, $y_1 = \sigma$; when $R/2 < x_1 \le R$, substituting the boundary conditions can be obtained:

$$x_1 = \frac{R}{2} \tag{1}$$

$$x_1 = R,\ y_1 = 0 \tag{2}$$

$$\int_0^{\frac{R}{2}} \sigma \mathrm{d}x_1 + \int_{\frac{R}{2}}^{R} \left(a_1x_1^2 + b_1x_1 + c_1\right)\mathrm{d}x_1 = \frac{1}{2}W \tag{3}$$

According to Marston theory, W is the vertical earth load per unit length of the tank cylinder structure and the calculation is given by the following equation:

$$W = \xi\, C_c\, \gamma\, D^2 \tag{4}$$

$$C_c = 1.4\frac{H_0}{D} \tag{5}$$

$$\xi = \frac{E}{E_d}\left(\frac{\delta}{R}\right)^3 \tag{6}$$

where C_c is the loading coefficient; ξ is the relative stiffness coefficient of the soil and the tank; γ is the heaviness of the soil; E is the elastic modulus of the tank; E_d is the elastic modulus of the soil; δ is the thickness of the tank wall; R is the radius of the tank.

Substitute into Eq. (3), get:

$$a_1 = \frac{36\sigma - 67.2\xi\gamma H_0}{R^2}, b_1 = \frac{100.8\xi\gamma H_0 - 56\sigma}{R}, c_1 = 20\sigma - 33.6\xi\gamma H_0$$

Thus the equation of the parabolic segment of vertical earth pressure is:

$$y_1 = \frac{36\sigma - 67.2\xi\gamma H_0}{R^2}x_1^2 + \frac{100.8\xi\gamma H_0 - 56\sigma}{R}x_1 + 20\sigma - 33.6\xi\gamma H_0 \tag{7}$$

Let the lateral earth pressure equation $q_{(h)}$ is $y_2 = a_2x_2^2 + c_2$, in the x_2–y_2 coordinate system, when $-R \le x_2 \le 0$, substituting the boundary conditions can be obtained:

$$x_2 = 0,\ y_2 = \sigma_h \tag{8}$$

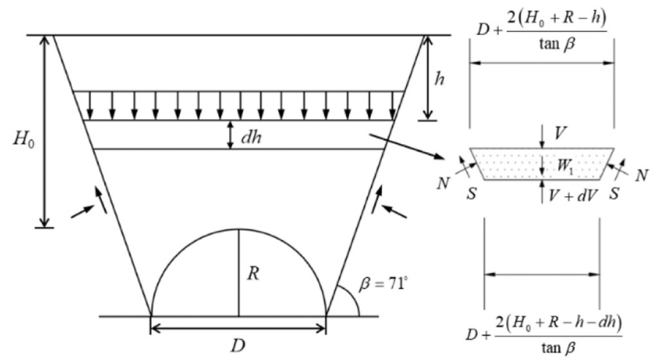

Fig. 3. "Marston inverted cone load" calculation model diagram.

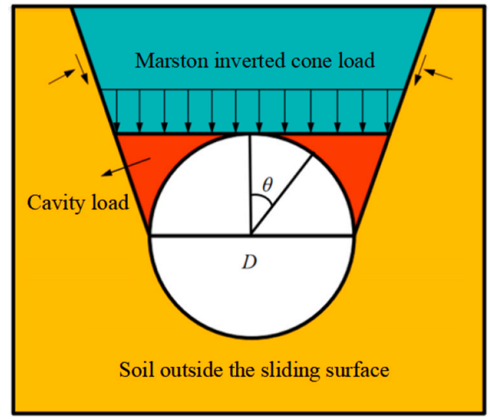

Fig. 4. Load calculation diagram of "inverted cone + tank cavity".

$$x_2 = -R,\ y_2 = 0 \tag{9}$$

get: $a_2 = -\frac{\sigma_h}{R^2}, c_2 = \sigma_h$.

The resulting parabolic equation for lateral earth pressure is:

$$y_2 = -\frac{\sigma_h}{R^2}x_2^2 + \sigma_h \tag{10}$$

Marston's theory [6] suggests that the soil above a cylindrical structure will form a soil column and will slip at the boundary with the adjacent soil, and that the width of the slipped soil column equals to the diameter of the structure. However, there are EEMUA 190 [5] international guidelines and a large number of scholars [17,18] who have found that the soil columns borne above the tanks are considered to be inverted conical with a slip surface that has a slip angle with the horizontal ground. Based on this, this section will derive the calculation method of soil load applicable to mounded storage tanks. The calculation model is shown in Fig. 3, in which the outer diameter of the storage tank is D, the radius is R, and the overburden height is H_0.

The force state of the soil unit inside the upper part of the storage tank is given in the figure at the same time, with the self-weight of the soil unit W_1, the height of the upper part of the unit from the surface of the soil layer as h. V and V+dV are the vertical forces at the top and the bottom of the soil unit, respectively, and N and S are the normal force and the shear force.

The weight of the soil unit is calculated as follows:

$$W_1 = \gamma\left(D + \frac{2(H + R_0 - h)}{\tan\beta}\right)\mathrm{d}h \tag{11}$$

Considering the equilibrium of the soil unit in the vertical direction, the following equations can be obtained:

$$W_1 = \mathrm{d}V + 2N\cos\beta + 2S\sin\beta \tag{12}$$

S is the sliding friction between the soil unit and the neighboring soil column; N is the lateral pressure of the neighboring soil column, which can be expressed as follows:

$$N = \sigma_n\frac{\mathrm{d}h}{\sin\beta} \tag{13}$$

$$S = \sigma_n\frac{\mathrm{d}h}{\sin\beta}\tan\phi \tag{14}$$

where σ_n is the normal stress at the interface between the soil unit and the adjacent soil column; ϕ is internal friction angle.

The vertical force V is shown below:

$$V = \sigma_v\left(D + \frac{2(H + R - h)}{\tan\beta}\right) \tag{15}$$

The vertical force increment dV is expressed below:

$$\mathrm{d}V = \left(D + \frac{2(H_0 + R - h)}{\tan\beta}\right)\mathrm{d}\sigma_v - \frac{2\sigma_v}{\tan\beta}\mathrm{d}h \tag{16}$$

Joint Eqs. (11–14) and (16) yield the following equation:

$$\gamma = \frac{\mathrm{d}\sigma_v}{\mathrm{d}h} + \frac{2\lambda}{D\tan\beta + 2(H + R - h)}\sigma_v \tag{17}$$

where the parameter λ is:

$$\lambda = I(\tan\beta\tan\phi + 1) - 1 \tag{18}$$

I is defined as the effect coefficient:

$$I = \frac{\sigma_n}{\sigma_v} \tag{19}$$

According to Marston theory, I is equal to the Rankine active earth pressure coefficient:

$$I = \tan^2\left(45 - \frac{\phi}{2}\right) \tag{20}$$

Solve Eq. (17) and consider the boundary condition, get:

$$\sigma_v = \frac{\gamma L}{2(\lambda - 1)}\left(1 - \frac{2h}{L}\right)\left[1 - \left(1 - \frac{2h}{L}\right)^{\lambda - 1}\right] \tag{21}$$

where the parameter L is:

$$L = D\tan\beta + 2(H_0 + R) \tag{22}$$

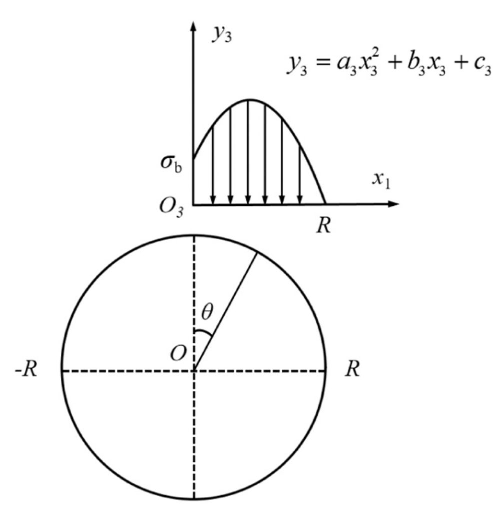

Fig. 5. Parabolic earth pressure model.

σ_v can be obtained from the top of the tank above the vertical load generated by the soil. However, due to the large diameter of the tank, an annular layer of cavity soil is distributed around the outer perimeter of the tank, and its "tank cavity" load contribution must be considered (Fig. 4). Assuming that the tank cavity soil is completely acting on the tank, the formula is:

$$\sigma_m = \gamma\left(\frac{7D^2}{12} - \frac{1}{2}\pi\frac{D^2}{4}\right)\Big/ D = 0.1906\gamma D \tag{23}$$

Due to the slippage between the soil and the tank and the position of the center of gravity of the soil, the soil pressure generated by the tank cavity load is not uniformly distributed, the maximum degree of action near the ends of the tank, near the top center of the tank when the role of the extent of the weakening. Therefore, for the characteristics of the tank's large diameter, the proposed "inverted cone + tank cavity" loading calculation method, the calculation formula is as follows:

$$\sigma = \begin{cases} \sigma_v + 0.1906\gamma D \sin\theta & (D > H) \\ \sigma_v & (D \le H) \end{cases} \tag{24}$$

When calculating the lateral earth pressure, σ_h is related to the "inverted cone + tank cavity" load:

$$\sigma_h = K_0\,\sigma \tag{25}$$

2.2. Mounded storage tanks earth pressure model on with angle = 0–90°

The earth pressure distribution on top of the tanks was analyzed using the numerical simulation results (Appendix B), which informed that the form of the earth pressure distribution was approximated as a "parabolic", and a new type of earth pressure calculation model was proposed based on this shape –the "parabolic" model (Fig. 5).

The model will be the upper part of the tank earth pressure is set to the vertical axis of the tank center as the axis of symmetry, from the top of the mid-point to the ends of the range of the quadratic parabolic distribution, the center of the tank for a certain value of σ_b, in the tank at the end of the horizontal diameter of both ends of the value of 0.

Let the equation of vertical earth pressure is $y_3 = a_3{x_3}^2 + b_3x_3 + c_3$, in the x_3–y_3 coordinate system, when $0 \le x_3 \le R$, substituting the boundary conditions gives:

$$x_3 = 0,\ y_3 = \sigma_b \tag{26}$$

$$x_3 = R,\ y_3 = 0 \tag{27}$$

$$\int_0^R a_3x_3^2 + b_3x_3 + c_3 = \frac{1}{2}W \tag{28}$$

Associatively Eqs. (26–28), get:

$$a_3 = \frac{3(\sigma_b - 2.8\gamma H_0)}{R^2}, b_3 = \frac{4(2.1\gamma H_0 - \sigma_b)}{R}, c_3 = \sigma_b.$$

Thus the equation for the vertical earth pressure on the side of the slope of mounded storage tanks is:

$$y_3 = \frac{3(\sigma_b - 2.8\gamma H_0)}{R^2}x_3^2 + \frac{4(2.1\gamma H_0 - \sigma_b)}{R}x_3 + \sigma_b \tag{29}$$

The top of the slope will lose a part of the soil, and the load generated by this lost part of the soil is defined as the side slope reduction load. Combining with the conclusion of the EEMUA 190 international guideline, and considering the existence of a large volume of thoracic soil in the cavity of the large-diameter tanks, we proposed the soil load calculation model applicable to the side of the side slope of the mounded storage tanks (Fig. 6), in which the radius is R, and the overburden height is H_0, the distance between the tanks and the distance between the tank and the start of the slope is L_1, the length of the slope reduction load is L_2, and the slope gradient is *i*. The relative positions of the Marston inverted cone load σ_v, the breastwork load σ_m, and the slope reduction load σ_i are also given in the figure.

As shown in Fig. 6, the distance L_1 between the center of the tank and the slope, and the length of the bottom edge L_2 of the slope to cut the triangular load are related to the overburden height H_0 and the radius R:

$$L_1 + L_2 = \frac{1}{3}H + R = \frac{1}{3}(H_0 + R) + R \tag{30}$$

If $L_2 > 0$, then $i = 0$ –90°.

Let the angle between the slope cut triangular load and the slope face of the slope be α. According to the law of triangles, the value of α is:

$$\alpha = 180^\circ - 71.6^\circ - i = 108.4^\circ - i \tag{31}$$

The value of the slope-cutting triangle load is related to the area of the triangle and is calculated as shown in Eq. (32):

$$\sigma_i = \gamma\left(2 \times \left(\frac{L_2}{2\sin\alpha}\right)^2 \sin\alpha \sin\beta \sin i\right)\Big/ R \tag{32}$$

From Marston theory, the lateral cutback load on the slope is given by:

$$\sigma_b = \sigma_v + \frac{1}{2}\sigma_m - \sigma_i \tag{33}$$

3. Model validation and parameter sensitivity analysis

3.1. Model validation

To validate the applicability of the proposed "cat-ear" and "parabolic" earth pressure models, the total pressure is obtained by synthesizing the vertical and lateral earth pressures, and the results of the "cat-ear" and "parabolic" models are compared with the results of the finite element analysis in terms of the overburden height and the diameter of the tank.

The results of the comparison between the "cat-ear" model and the finite element are shown in Fig. 7. It can be seen that the overall fit of the model to the finite element results reaches a maximum at the tank diameter of 5 m and the overburden height of 2 m. With the increase of the overburden height, the growth of earth pressure in the middle region of the model is gentle, and the influence of the tank cavity load is reduced. Tables 1 and 2 demonstrate the maximum and average earth pressure results, respectively. In terms of maximum earth pressure, calculations from the "cat-ear" model are 0.99–1.16 times those obtained from finite element analysis; in terms of average earth pressure, they are 1.03–1.09 times. Fig. 8 shows the corresponding comparison between the "parabolic" model and finite element analysis. It can be seen that with the increase of the overburden height, the location of the

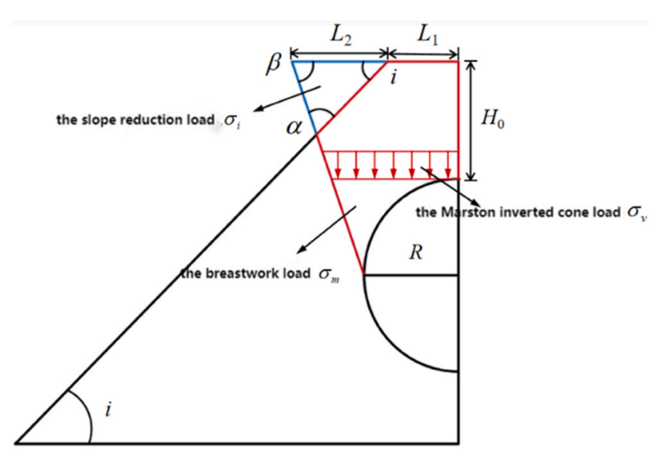

Fig. 6. Marston inverted cone + thoracic discounted load calculation model diagram.

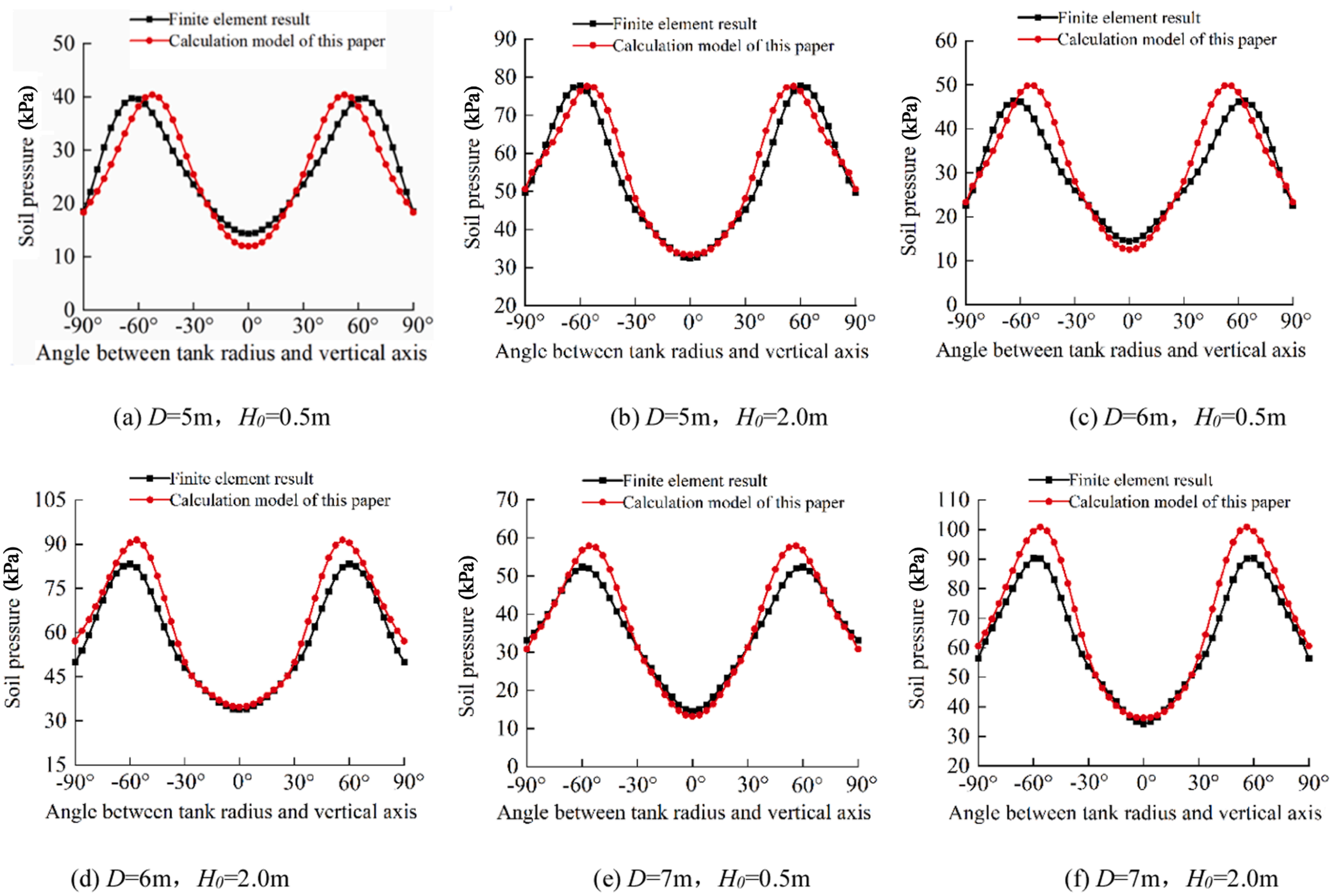

Fig. 7. Comparison of earth pressure for various tank diameters and overburden heights with angle = 90°.

Table 1
Comparison of maximum earth pressures for “cat-ear” and “parabolic” models with finite element results.

Typology	Overburden heights (m)	Comparison of maximum earth pressure			
		Diameter 5 m	Diameter 6 m	Diameter 7 m	Diameter 8 m
“Cat-ear” model/ finite element results	0.5	1.05	1.10	1.13	1.16
	2.0	1.01	1.08	1.11	1.12
	4.0	0.99	1.05	1.09	1.09
“Parabolic” model/ finite element results	0.5	0.95	1.07	1.17	1.22
	1.0	1.07	1.09	1.13	1.16
	2.0	1.16	1.12	1.09	1.05
	3.0	1.22	1.15	1.04	0.97

Table 2
Comparison of average earth pressures for “cat-ear” and “parabolic” models with finite element results.

Typology	Overburden heights (m)	Comparison of average earth pressure			
		Diameter 5 m	Diameter 6 m	Diameter 7 m	Diameter 8 m
“Cat-ear” model/ finite element results	0.5	1.04	1.06	1.04	1.08
	2.0	1.03	1.08	1.07	1.03
	4.0	1.04	1.09	1.04	1.03
“Parabolic” model/ finite element results	0.5	0.97	1.02	1.07	1.11
	1.0	0.94	0.97	1.02	1.05
	2.0	0.90	0.93	0.95	0.97
	3.0	0.84	0.87	0.90	0.92

maximum earth pressure obtained tends to overlap. The values of earth pressure at the two ends of the horizontal diameter of the tank have a certain degree of disparity due to the increase in lateral pressure on the tank. This makes the earth pressure in the rising section of the “parabolic” model less than the finite element results, and the fit is better in the falling section of the parabola. The maximum and average earth pressure results are shown in Tables 1 and 2. In terms of maximum value, the “parabolic” model produces results 0.95–1.22 times the finite element results; in terms of average earth pressure, it produces results 0.84–1.11 times. In general, the “cat-ear” and “parabolic” earth pressure distribution models fit well with the finite element results and can basically cover the earth pressure calculations for tanks with low overburden heights, high overburden heights and various diameters.

3.2. Sensitivity analysis

The earth pressure on the covered cylinder structure at the slope position is mainly related to the height of the covered soil, the slope, and the distance between the structure and the slope. Therefore, selects the above factors for sensitivity analysis. Taking the tank diameter D= 5 m, overburden height H= 2 m as the research object, the distribution of earth pressure on the top of the mounded storage tank with different slope angles i was analyzed and sensitivity analysis was carried out by changing D (5, 6, 7, 8 m) and H (0.5, 2, 4 m; 0.5, 1, 2, 3 m).

The distribution of earth pressure under each parameter is shown in Fig. 9. From Fig. 9a-b, the earth pressure of tanks with angle = 90° is distributed in a “concave” shape. The earth pressure on the top of the

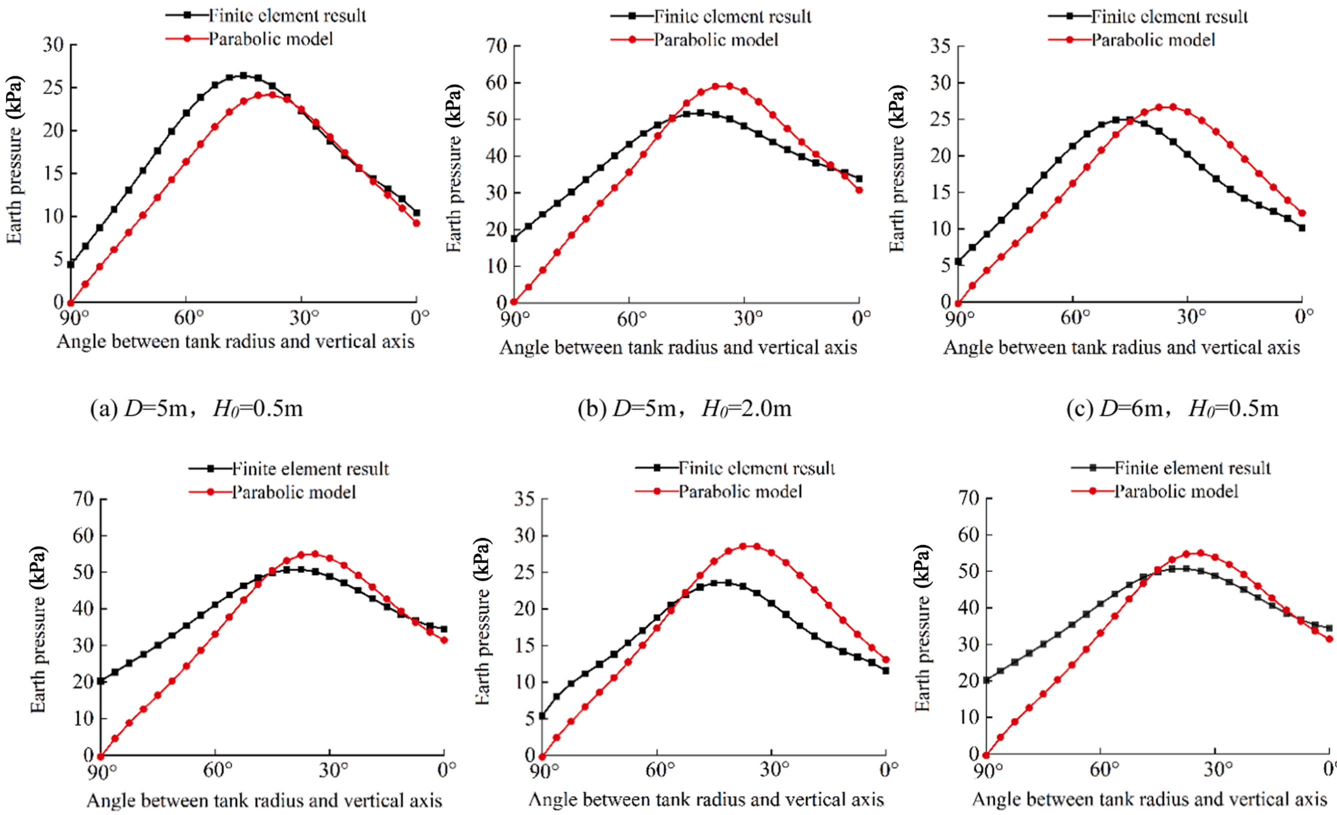

(a) D=5m, H_0=0.5m (b) D=5m, H_0=2.0m (c) D=6m, H_0=0.5m

(d) D=6m, H_0=2.0m (e) D=7m, H_0=0.5m (f) D=7m, H_0=2.0m

Fig. 8. Comparison of earth pressure for various tank diameters and overburden heights with angle = 45°.

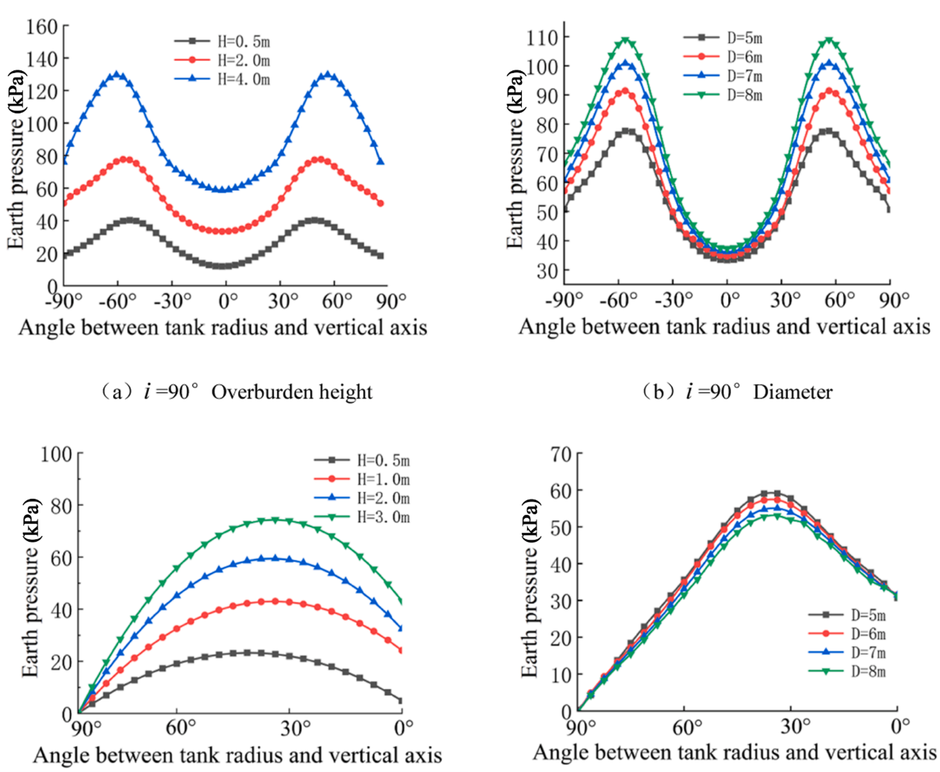

(a) i =90° Overburden height (b) i =90° Diameter

(c) i=45° Overburden height (d) i=45° Diameter

Fig. 9. Parameter sensitivity analysis.

tanks grows slowly in the center area (θ =0°–30°), and then it starts to increase dramatically in the range of 30°–60°, with the maximum value appearing at the position of θ about 60°, followed by a gradual decrease. With the increase of overburden height, the overall earth pressure is upward trend, the maximum value reaches 130 kPa at a height of 4 m; with the increase of the tank diameter, the location of the maximum soil pressure value of the tank is gradually converging to the center of the tank, and the minimum earth pressure of the tank and the difference between the earth pressure value of the two ends of the tank increases, which is due to the fact that the bigger the diameter of the tank body, the larger the area of tank body contact with the soil, increasing the tank cavity load and the lateral pressure at the ends of the tank. Meanwhile, the larger the diameter of the tank, the greater the maximum difference in earth pressure values. As can be seen from Fig. 9c-d, the earth pressure of tanks with angle = 45° has an overall "parabolic" distribution. After increasing the height, the earth pressure of the tank on the side of the slope increases, but the growth rate is smaller than that of the non-slope side. The earth pressure of the tank on the side of the slope is reduced by the increase in tank diameter. This is due to the presence of a cavity load at the top of the tank on the side of the slope, where the earth pressure is less than the earth pressure on the non-slope side of the tank. An increase in tank diameter results in the tank being closer to the side of the slope, the tank cavity load decreases, and the tank earth pressure decreases.

4. Conclusions

With the continuous expansion of deep resource exploitation and underground space utilization, deep underground energy storage engineering, underground petroleum reserve engineering, and concealed hazardous chemical storage engineering have imposed higher demands on the safe design of covered structures. Large-diameter mounded horizontal tanks are an important structural form in such engineering systems, and their earth pressure distribution is jointly affected by cover depth, tank diameter, and slope angle, showing significant large-diameter and slope effects. Therefore, the investigation of earth pressure calculation methods for large-diameter mounded tanks under different slope angles is of considerable engineering significance. Based on this, the main conclusions of this study are as follows:

(1) A new type of earth pressure model comprising "cat-ear" model and "parabolic" model is proposed for mounded storage tanks with a diameter of not less than 5 m and an overburden height of more than 0.5 m. The load is calculated using the method of "inverted cone + tank cavity".
(2) A parameter sensitivity analysis was performed for the model with tank diameter and overburden height. It was shown that the addition of overburden height increases the earth pressure, which increases slowly for slopes i = 0–90° compared to i = 90°; the increase in tank diameter increases the earth pressure at i = 90° but the opposite is true at i = 0–90°.
(3) In comparison with the finite element results in the appendix, the "cat-ear" model gives results 0.99–1.16 times the finite element results, and the "parabolic" model 0.95–1.22 times. The earth pressure distribution and size of the model can cover a variety of overburden height and tank diameter, with high calculation accuracy and good applicability, which can provide reference for the structural design of mounded storage tanks and the formulation of specifications.

CRediT authorship contribution statement

Zheng Nie: Formal analysis, Conceptualization. **Yu Zhang:** Project administration. **Shengjie Di:** Conceptualization. **Chongqun Gao:** Software. **Jiawei Lu:** Validation. **Jiajun Liu:** Methodology.

Declaration of Competing Interest

We, [Zheng Nie, Yu Zhang, Shengjie Di, Chongqun Gao, Jiawei Lu, Jiajun Liu], the authors of the manuscript titled **"Calculation model of overburden pressure of large diameter mounded storage tanks under different overburden slope angles"**, declare that we have no financial or personal relationships with other people or organizations that could inappropriately influence our work. There are no potential conflicts of interest relevant to this manuscript. All authors have reviewed and approved this declaration.

Acknowledgments

This work was supported by funding from the National Natural Science Foundation of China (Grant No. 51890914, 52179119), Natural Science Foundation of Liaoning Province (Grant No. 2024-MSBA-47), Natural Science Basic Research Project of Shaanxi Province (Grant No. 2024JC-YBQN-0357), Key research and development projects in Shaanxi Province (Grant No. 2025CY-YBXM-466). The authors would like to acknowledge Mr. Mingze Jia and the China University of Petroleum (East China) for their valuable contributions made during Mr. Jia's graduate studies, as well as Mrs. Yalin Luan of China University of Petroleum (East China) for her extensive participation in the manuscript revision and substantial contributions to its improvement.

When conducting finite element calculations, the following assumptions exist:

(1) The influence of the redistribution of stress around the storage tank due to the change of the original equilibrium stress field caused by the compaction of backfill soil and the existence of the tank structure is ignored. The tank model is a regular cylindrical structure with end caps, and the influence of auxiliary structures such as the bottom channel is ignored.
(2) The upper part of the soil model is a free boundary and no additional loads are applied. Since the initial stress balance has been set, the effect of soil pressure on the storage tank after soil compaction is achieved by directly applying gravity loads during the simulation.
(3) Normal displacement constraints are applied to the left and right as well as the front and rear end faces of the soil model to simulate the normal displacement restrictions on the soil by adjacent soil.

Appendix A

Finite element calculation of earth pressure storage tanks with angle = 90°

Tank-overburden ABAQUS finite element calculation model is shown in Fig. A.1. A three-dimensional model is adopted for the calculation. As the overburden tank structure is symmetric in the front and back direction, this paper uses 1/2 model symmetry analysis. Tank size and L/D ratio in accordance with EEMUA 190 international guidelines to determine the height of the overburden height H_0, tank diameter D, length 8D, tank bottom from the bottom of the soil 0.5D, wall thickness of 50 mm, the head for the hemisphere, the soil model for the length of 5D, the width of 3D, the model of the bottom of the fixed constraints, front and rear and left and right end face of the displacement constraints along the normal direction, the top surface is free, fixed boundaries within 120° of the lower half of the tank to simulate the support of a sand bed. The tank is simulated by a curved fournode thin-shell unit S4R, and the soil is simulated by a three-dimensional eight-node solid unit C3D8R. The modulus of elasticity of the tank material is 206 GPa, Poisson's ratio is 0.28, density is 7850 kg/m^3, and the plasticity parameters are modeled by triple folding line. The soil samples were taken from the in-situ soil at the construction site of a large domestic hazardous chemical mounded storage tank, whose composition is close to that of powdery clay. The initial parameters used in the model are shown in Table A.1.

In this paper, the classical M-C model is used for the finite element soil constitutive model. Considering the interaction between the storage tank and surrounding soil, surface-to-surface contact pairs are established between the tank outer wall and soil mass in the finite element model. The tank wall with higher stiffness is defined as the master surface, while the soil with lower stiffness is set as the slave surface. The Coulomb friction model is adopted to characterize the interfacial mechanical behavior of contact pairs. Finite sliding is selected as the contact slip formulation, and the penalty friction algorithm is utilized with a friction coefficient of 0.25. Gravity loads are applied directly to reproduce the earth pressure effect generated by compacted soil on the storage tank.

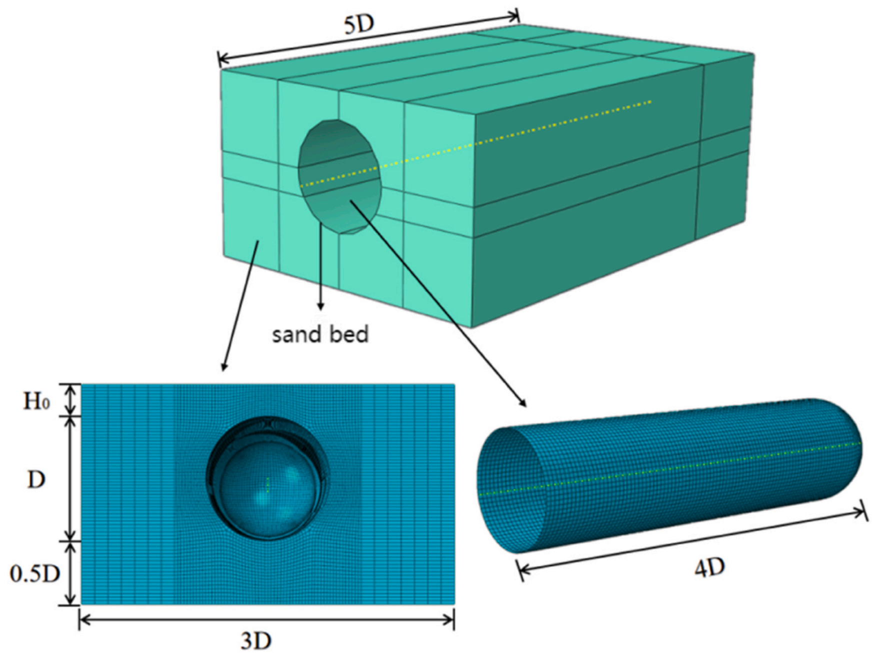

Fig. A.1. Finite element model.

Table A.1
Material parameters of soil and storage tank.

Parameters	Numerical value	Parameters	Numerical value
Tank Initial yield stress	345 MPa	Soil density	1800 kg/m^3
Tank Initial plastic strain ε_0	0	Cohesion	15 kPa
Tank First yield stress σ_1	439 MPa	Internal friction angle	30°
Tank First plastic strain ε_1	0.0474	Soil deformation modulus	10 MPa
Tank Second yield stress σ_2	582 MPa	Soil poisson's ratio	0.35
Tank Second plastic strain ε_2	0.1377	Soil shear angle	0
Tank third yield stress σ_3	625 MPa	Tank third plastic strain ε_3	0.18

Taking the mounded storage tanks with diameters D of 5, 6, 7 and 8 m as the research objects, the effects of overburden height and tank diameter on earth pressure are analyzed in depth. The finite element model interface is selected as the research section, and the earth pressure can be obtained from the contact pressure between the soil body and the tank wall obtained by finite element calculation. The overburden height H_0 is taken as 0.5, 1, 2, 3, 4 and 5 m.

Fig. A.2 illustrates the distribution of vertical earth pressure under tanks with various diameters and different overburden depths. It can be observed that the earth pressure on the crown of tanks with four different diameters exhibits an approximately concave distribution under various overburden depths. The minimum earth pressure occurs directly above the tank central apex rather than at the two ends along the horizontal diameter of the tank (hereinafter referred to as the tank ends). With the rise in overburden depth, the concave characteristic of earth pressure distribution at the tank center becomes more prominent, and the distribution curve gradually tends to be M-shaped. The earth pressure within the circumferential range of 30°–90° presents an evident parabolic distribution. In addition, as the tank diameter increases, the position corresponding to the maximum earth pressure gradually shifts toward the tank center. Meanwhile, the difference between the minimum earth pressure at the tank crown and the earth pressure at the tank ends enlarges. This phenomenon can be attributed to the fact that a larger tank diameter leads to a larger contact area between the tank and surrounding soil, which further increases the load induced by the tank cavity. Consequently, the lateral earth pressure at the tank ends becomes higher. Furthermore, the disparity in the maximum earth pressure value grows with increasing tank diameter.

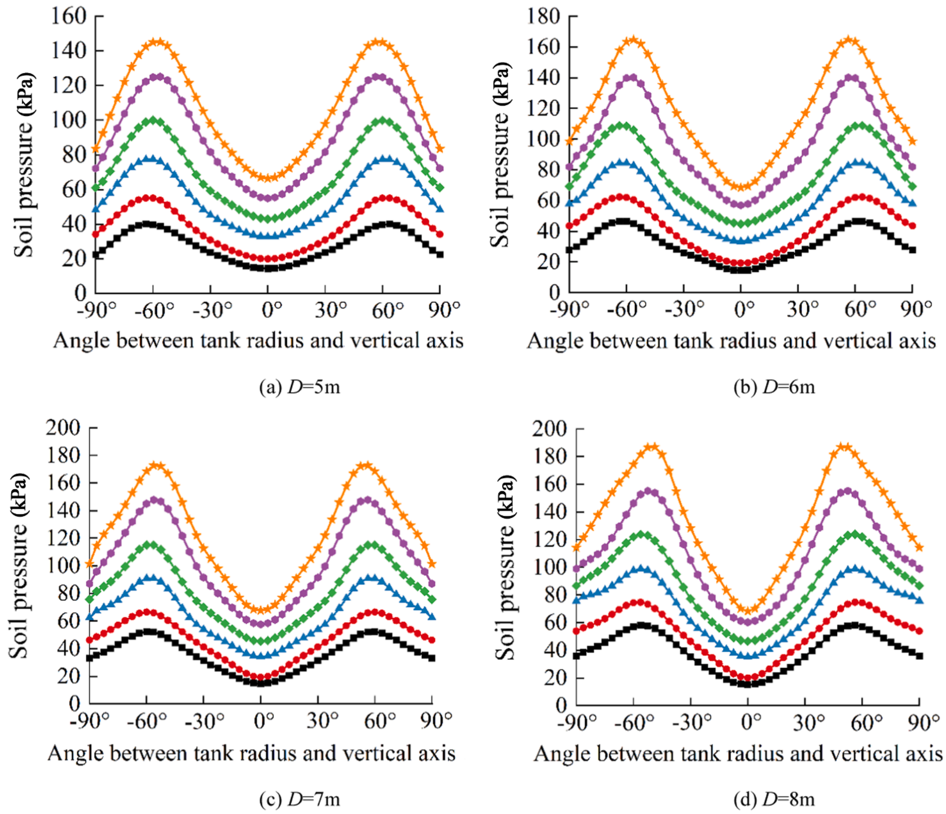

Fig. A.2. Earth pressure distribution for different diameters D and overburden heights H_0.

Appendix B

Finite element calculation of earth pressure storage tanks with angle = 0–90°

The tank-overburden-slope ABAQUS finite element calculation model is shown in Fig. B.1, and the 3D model is selected for the calculation and analyzed symmetrically using 1/2 model. Where Fig. B.1a represents the soil body of the slope, Fig. B.1b is the top view of the soil body at the position of the tank head, Fig. B.1c is the front view of the soil body, and Fig. B.1d is mounded storage tanks, and the relative position of the soil body is shown in the figure.

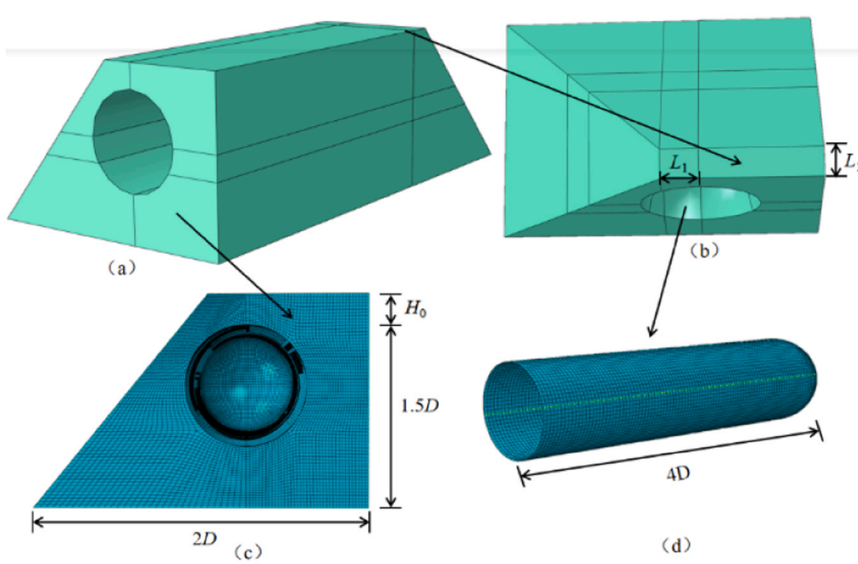

Fig. B.1. Finite element model.

The slope and the top surface of the soil body are set as free boundaries, the bottom surface of the soil body is a fixed constraint, and the right side surface is set as a normal constraint. The specific dimensions of the model are shown in Fig. B.1. The parameters of soil and tank are consistent with Appendix A.

The storage tanks with diameters of 5, 6, 7 and 8 m were selected as the objects of study, and the overburden height H_0 was set to 0.5, 1, 2 and 3 m. An in-depth analysis was conducted on the effects of overburden height and tank diameter on earth pressure.

Fig. B.2 presents the earth pressure distributions for tanks under different overburden heights and diameters. It can be observed that the magnitude and distribution pattern of earth pressure on the non-slope side (i.e., the right side of the tank in the simulation) are basically consistent with the results presented in Appendix A. This demonstrates that the influence of the slope on the non-slope side of the tank is extremely small and can be neglected. However, the earth pressure on the slope side (i.e., the left side of the tank in the simulation) changes significantly under the effect of the slope.

When the overburden height $H_0 = 0.5$ m, the earth pressure on the slope side follows a parabolic distribution. Compared with the non-slope side, the region of parabolic earth pressure distribution on the slope side is closer to the centre of the tank top, as reflected by the position of the maximum earth pressure. As the tank diameter increases, the location of the maximum earth pressure on the slope side shifts toward the tank centre. This is attributed to the varying distance between the tank centre and the slope: a larger tank diameter corresponds to a thinner overlying soil layer on the slope side, which generates lower soil pressure. On the other hand, the non-slope side is subjected to full earth pressure. As the tank diameter increases, the contact area between the tank and soil expands, leading to higher earth pressure. With rising overburden height, the earth pressure on the slope side generally increases, but its growth rate is lower than that on the non-slope side.

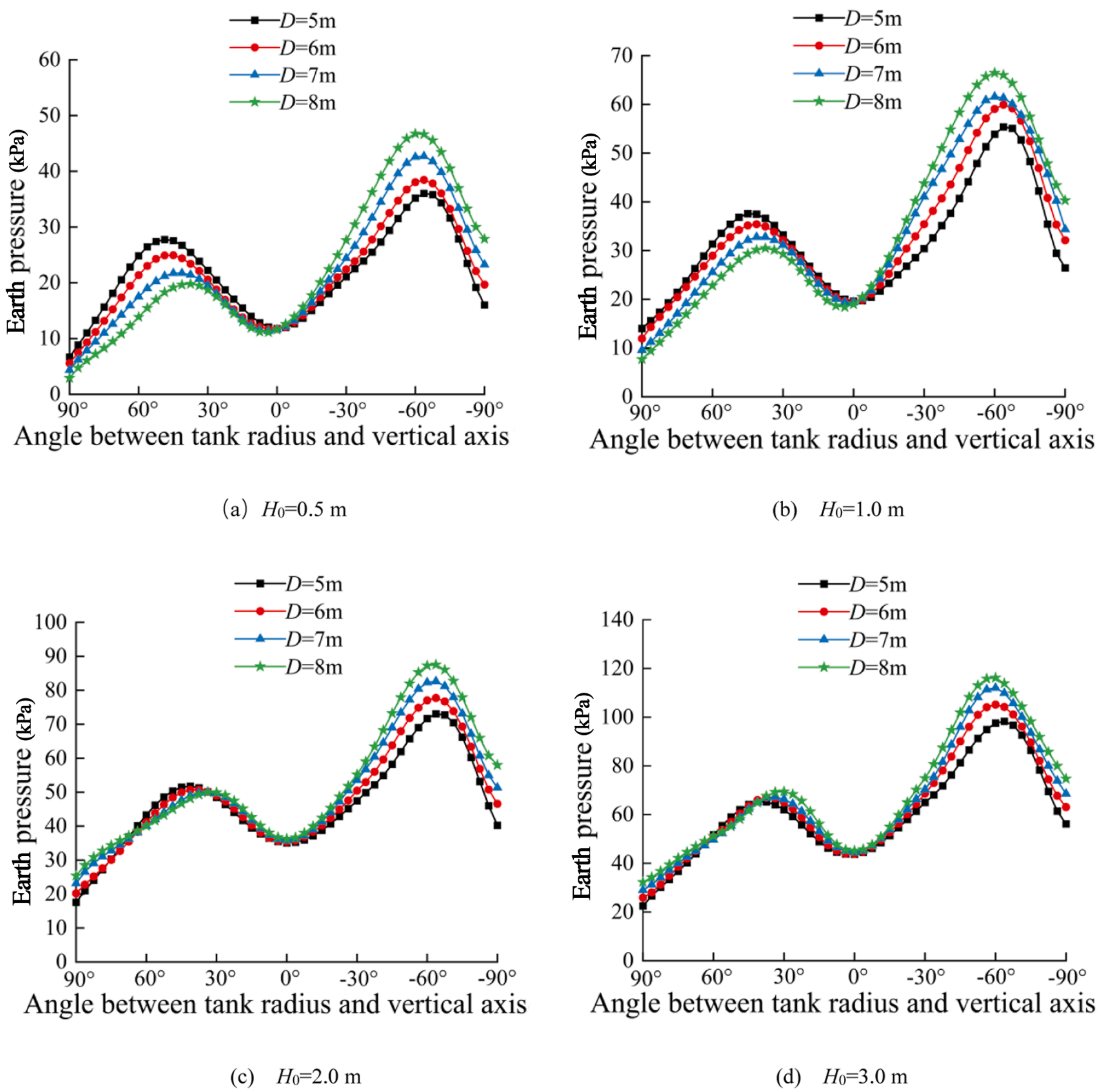

Fig. B.2. Distribution of earth pressure in tanks with different overburden heights and tank diameters.

The maximum and average earth pressures on the slope side of the storage tank were compared to the non-slope side, as shown in Fig. B.3.

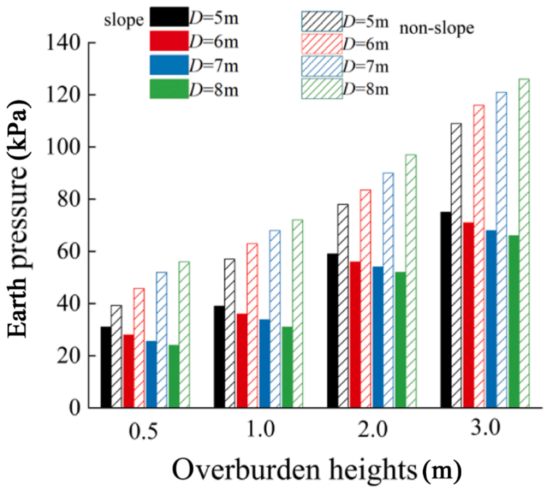

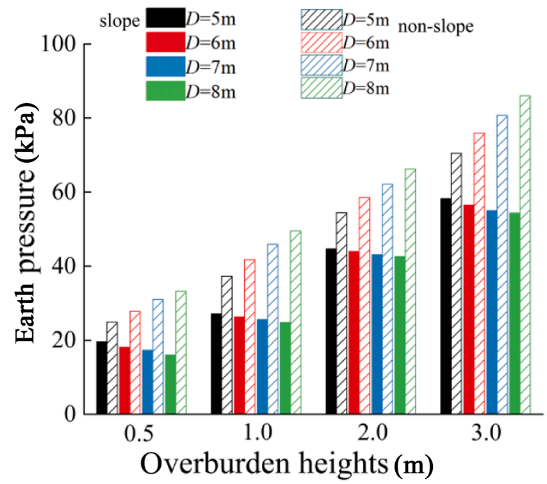

Fig. B.3. Comparison of earth pressure on the slope side and non-slope side of tanks with different overburden heights.

From Fig. B.3, it can be seen that the larger the diameter of the tank, the more uniform the distribution of earth pressure on the slope side compared to the non-slope side, and the reduction of the maximum and average values of earth pressure is more conducive to the force stability of the tank. After increasing the overburden height, the earth pressure on the slope side of the tank increases, but the growth is smaller than the non-slope side. In summary, the increase in the overburden height will increase the earth pressure on the slope side of the tank, while the increase in the tank diameter will reduce the earth pressure on the slope side.

Data availability statement

The data that has been used is confidential.

References

[1] G. Tao, C. Zhao, C. Liu, et al., Consequence analysis and simulation calculation of LPG tank car explosion accident, J. Saf. Environ. 26 (3) (2026) 933–938 (in Chinese).
[2] X.M. Guo, P. Mei, Research on the technical framework of data flow anomaly detection for major hazard sourcandes in tank farm, Sci. Technol. Innov. (15) (2018) 66–67+69 (in Chinese).
[3] T. Wang, W. Xia, Construction techniques of mounded vessels for pressurized storage of liquefied hydrocarbons at ambient temperature, Pet. Eng. Constr. 46 (4) (2020) 51–57 (in Chinese).
[4] W. Xia, Design and application of mounded storage tank for pressurized storage of liquefied hydrocarbon at ambient temperature, Pet. Eng. Constr. 44 (3) (2018) 1–6 (in Chinese).
[5] EEMUA 190, Guide for the design, construction and use of mounded horizontal cylindrical vessels for pressurized storage of LPG at ambient temperatures, 2017.
[6] A. Marston, A.O. Anderson, The theory of loads on pipes in ditches and tests of cement and clay drain tile and sewer pipe, Bulletin 31, Iowa Engineering Experiment Station, Ames, Iowa, USA, 1913.
[7] American Water Works Association, Steel pipe: A guide for design and installation, 2017.
[8] I. Shmulevich, N. Galili, A. Foux, Soil stress distribution around buried pipes, J. Transp. Eng. 112 (5) (1986) 481–494.
[9] W.M. Shen, X.C. Bian, X.W. Tang, et al., Model tests and theoretical studies on earth pressure on shallow positive buried culverts, Chin. J. Geotech. Eng. 32 (7) (2010) 1017–1022 (in Chinese).
[10] T. Kawabata, H.I. Ling, Y. Mouri, et al., Behavior of buried flexible pipe under high fills and design implications, J. Geotech. Geo-Environ. Eng. 132 (10) (2006) 1354–1359.
[11] T. Kawabata, Y. Mouri, H. Tamura, et al., Field test for buried large steel pipes with thin wall, in: Pipelines 2006: Service to the Owner, Chicago, Illinois, USA, 2006.
[12] Z.F. Zhou, J.M. Ling, B. Liang, Analysis of earth pressure on oil pipe, J. Chongqing Jiao Tong Univ. (Nat. Sci.) 30 (4) (2011) 794–797 (in Chinese).
[13] Z.F. Zhou, J.M. Ling, B. Liang, et al., Analysis on additional stress for apron oil pipe under external loads, J. Tongji Univ. (Nat. Sci.) 41 (8) (2013) 1219–1224+1262 (in Chinese).
[14] J.H. Yu, C.Z. Shi, H.G. Wu, et al., Soil pressures at top of large-diameter buried steel pipes and their design model, Chin. J. Geotech. Eng. 44 (3) (2022) 514–522 (in Chinese).
[15] X. Wang, Design of buried horizontal storage tank, J. Shandong Ind. Technol. (2) (2015) 49–50 (in Chinese).
[16] M.U.A. Khan, S.K. Shukla,, T.S. Paraskeva, Stress distribution around the conduit buried within a soil slope - an experimental investigation, Transp. Geotech. 32 (2022) 100687.
[17] B. Huang, J.W. Liu, D.S. Ling, et al., Application of particle image velocimetry (PIV) in the study of uplift mechanisms of pipe buried in medium dense sand, J. Civ. Struct. Health Monit. 5 (5) (2015) 599–614.
[18] K. Roy, B. Hawlader, S. Kenny, et al., Upward pipe–soil interaction for shallowly buried pipelines in dense sand, J. Geotech. Geoenviron. Eng. 144 (11) (2018) 04018078.

Yu Zhang is a professor and a supervisor for Ph.D. students. In 2007, 2012, and 2014, he obtained a bachelor's degree from Hohai University, a Ph.D. degree from Hohai University, and a Ph.D. degree from the Université de Lille in France, respectively. His research focuses on the field of deep-seated oil and gas resource exploitation and storage. He has presided over general and youth projects of the National Natural Science Foundation of China, collaborative research tasks of national major projects, general and youth projects of the Shandong Provincial Natural Science Foundation, and Qingdao's applied basic research projects. He has published more than 60 high-level papers in SCI and EI-indexed journals as the first or corresponding author, and some of his papers have been selected for the F5000 – Top Academic Papers in China's High-quality Scientific and Technical Journals. He has been granted 10 invention patents, with an industrial transformation value of 1.12 million yuan. He has won one first-class prize for scientific and technological progress in Qingdao, two third-class prizes for scientific and technological progress in Shandong Province, and one first-class prize for scientific and technological progress from the China Petroleum and Chemical Industry Federation. He has been rated as a "High-level and Scarce Talent (Zhidao Plan)" in Qingdao and has received the Outstanding Young Scientist Award in the field of Mining, Petroleum, and Safety Engineering in Chinese Universities. Currently, he serves as a committee member of the Multi-field Coupling of Rock and Soil Mass Specialty Committee of the Chinese Society for Rock Mechanics and Engineering, a committee member of the Specialty Committee of Rock Mechanics and Engineering for Low-carbon Energy, a council member of the Shandong Society for Rock Mechanics and Engineering, and an executive editor-in-chief of *Acta Petrolei Sinica*.